

Distances of Dwarf Carbon Stars

HUGH C. HARRIS,¹ CONARD C. DAHN,¹ JOHN P. SUBASAVAGE,¹ JEFFREY A. MUNN,¹
BLAISE J. CANZIAN,² STEPHEN E. LEVINE,³ ALICE B. MONET,¹ JEFFREY R. PIER,¹
RONALD C. STONE,^{1,*} TRUDY M. TILLEMANN,¹ AND WILLIAM I. HARTKOPF⁴

¹*US Naval Observatory, Flagstaff Station, 10391 W. Naval Observatory Road, Flagstaff, AZ 86005-8521, USA*

²*L-3 Communications/Brashear, 615 Epsilon Dr., Pittsburgh, PA 15238-2807, USA*

³*Lowell Observatory, 1400 W. Mars Hill Road, Flagstaff, AZ 86001-4499, USA*

⁴*US Naval Observatory, 3450 Massachusetts Ave. N. W., Washington, DC 20392-5420, USA*

ABSTRACT

Parallaxes are presented for a sample of 20 nearby dwarf carbon stars. The inferred luminosities cover almost two orders of magnitude. Their absolute magnitudes and tangential velocities confirm prior expectations that some originate in the Galactic disk, although more than half of this sample are halo stars. Three stars are found to be astrometric binaries, and orbital elements are determined; their semimajor axes are 1–3 AU, consistent with the size of an AGB mass-transfer donor star.

Keywords: astrometry, parallaxes, proper motions, stars: distances, stars:carbon

1. INTRODUCTION

Distances, absolute magnitudes, and luminosities for the dwarf carbon (dC) stars are uncertain. They tend to be faint, and at sufficiently large distances, that parallaxes are not easy to measure. To date only three have published parallaxes (Dahn et al. 1977; Harris et al. 1998); those three have similar colors and absolute magnitudes. However, properties of the many dwarf carbon stars discovered in recent years (Margon et al. 2002; Downes et al. 2004; Green 2013) suggest that they are likely to have a broad range of physical properties, and expectations about their origin (Green & Margon 1994) suggest that they are likely to be produced in both disk and halo populations with a

range of metallicities and absolute magnitudes. This paper presents parallaxes for an expanded sample of dwarf carbon stars, with a goal of investigating the range of absolute magnitudes over which these stars extend.

2. DATA

2.1. *Sample*

The sample of 20 dC stars in this paper consists of 13 targets taken from the Sloan Digital Sky Survey (SDSS; Fukugita et al. 1996; Gunn et al. 1998, 2006; York et al. 2000) and seven targets from other papers in the literature. Three have parallaxes published previously (Harris et al. 1998), and here we give an improved parallax for two of them (LHS 1075 and CLS 96), and an entirely new parallax for the third (G77-61). These targets were chosen to be definite dwarfs (as opposed to giant carbon stars) based on their significant proper motions. They were selected to be “nearby”

Corresponding author: Munn, J. A.
jam@nofs.navy.mil

* Deceased

(with distances likely to be within 300 pc) so as to have significant parallaxes; criteria used to select the sample included large proper motion, bright apparent magnitude for a candidate’s color, and a range of colors and band strengths so as to include a variety of types of stars. The sample does not include any of the warm, CH-like stars from the SDSS, because the estimated distances for even the brightest were > 500 pc, too distant to get a meaningful parallax measurement.

2.2. Astrometry

Images have been taken with the U.S. Naval Observatory’s (USNO) 1.55 m Strand Astrometric Reflecting Telescope in Flagstaff, AZ. Descriptions of the telescope, the CCD cameras and filters used here, and the observing and processing procedures are given by [Monet et al. \(1992\)](#) and [Dahn et al. \(2017\)](#). The astrometric results are given in Table 1. Column (1) gives the identifying number in the 2MASS Point Source Catalog ([Skrutskie et al. 2006](#)). The 2MASS J number provides an unambiguous link to SIMBAD where many alternate names and much additional information can be found. Column (2) gives alternate names, usually the name by which the star was first identified as a carbon star. Columns (5) and (6) indicate the camera and filter employed for each parallax determination, while Columns (7), (8), and (9) give the number of acceptable CCD frames (observations), the number of separate nights on which those observations were obtained, and the number of reference stars employed in astrometric solutions, respectively. Columns (10) and (11) give the years observed and total epoch range, respectively. The derived relative parallax and its mean (standard) uncertainty are given in Column (12) (throughout this work we refer to the trigonometric parallax angle as π). The relative total proper motion and its uncertainty follow in Column (13), and the position angle of the proper motion is given in Column

(14). The error in the position angle reflects the uncertainty in the orientation of the CCD in its dewar, and of the dewar on the telescope. The derived absolute parallax and its uncertainty are presented in Column (15), and the calculated tangential velocities and their uncertainties are given in Column (16).

Many of the 20 stars in this paper are near the faint limit for this observing program and require long exposure times and good seeing. As a consequence, we have obtained fewer observations than desired, some with lower signal-to-noise ratio than desired, and the resulting parallax values have larger errors than desired. Nevertheless, the parallaxes are significant for all stars: the fractional error in parallax has a median value of 9%, and ranges from 3% in the best case to 23% in the worst case.

2.3. Photometry

Photometry of most of the target stars and their surrounding reference stars was obtained with the USNO 1.0 m and 1.55 m telescopes using Johnson-Cousins *BVI* filters. These data were used in the astrometric processing above to correct for differential color refraction (DCR). For those fields lacking *BVI* photometry, *gri* data from the SDSS database were transformed to *BVI* using the relations of [Ivezić et al. \(2007\)](#) and then used for the DCR corrections. Photometric data for the 20 dC target stars is given in Table 2 including *JHK_S* from 2MASS.

2.4. Binary Orbits

Three stars in this sample, LSPM J0742+4659, LP225-12, and LP758-43, were found to have significant systematic astrometric residuals from the default solution for parallax and proper motion, indicating a periodic perturbation from an unseen binary companion. A solution for the orbit of the photocenter (iterating between the parallax solution with the orbit removed, and the orbit solution with the parallax and proper motion removed) was carried

Table 1. Astrometric Results

2MASS J	Alternate Names	R.A. ^a	Decl. ^a	Cam.	Filt.	Nf	Nn	Ns
(1)	(2)	(J2000.0)	(4)	(5)	(6)	(7)	(8)	(9)
00260048-1918519	LHS1075 (LP765-18)	00 26 00.2	-19 18 52	TEK2K	A2-1	148	129	7
01202853-0836307	SDSS J012028.55-083630.8	01 20 28.5	-08 36 31	EEV24	I-2	112	92	10
01215031+0113024	LP587-45 (NLTT4523)	01 21 50.3	+01 13 03	TEK2K	I-2	145	144	8
03323808+0157599	G77-61 (LHS1555)	03 32 38.1	+01 58 00	EEV24	A2-1	117	71	13
07425720+4659186	LSPM J0742+4659	07 42 57.2	+46 59 18	EEV24	I-2	277	145	12
08180742+2234290	SDSS J081807.45+223427.6	08 18 07.4	+22 34 29	EEV24	I-2	127	106	20
08345114+0740088	SDSS J083451.15+074008.8	08 34 51.2	+07 40 09	EEV24	A2-1	37	30	17
09332463-0031445	HE 0930-0018	09 33 24.6	-00 31 45	TEK2K	A2-1	100	97	14
10542941+3402259	CLS31	10 54 29.4	+34 02 26	EEV24	I-2	63	61	9
11203487+5559373	SDSS J112034.86+555937.2	11 20 34.9	+55 59 37	TEK2K	I-2	204	186	7
13533300-0040395	SDSS J135333.01-004039.4	13 53 33.1	-00 40 40	TEK2K	I-2	222	198	11
14531880+6004209	SDSS J145318.83+600421.0	14 53 18.8	+60 04 21	EEV24	I-2	111	93	9
14572597+2341257	SDSS J145725.86+234125.5	14 57 26.0	+23 41 26	EEV24	I-2	44	41	21
15270276+4345172	SDSS J152702.74+434517.3	15 27 02.8	+43 45 17	TEK2K	I-2	287	231	15
15480927+3227247	SDSS J154809.22+322724.9	15 48 09.2	+32 27 25	TEK2K	I-2	115	96	15
15523734+2927591	LP328-57 (CLS96)	15 52 37.4	+29 27 59	TEK2K	A2-1	242	183	10
16223288+4237538	LP225-12 (NLTT42660)	16 22 32.9	+42 37 54	TEK2K	I-2	293	231	8
16313278+3553285	LP275-54 (NLTT43012)	16 31 32.8	+35 53 29	EEV24	I-2	147	106	17
21051653+2514486	LSR J2105+2514	21 05 16.5	+25 14 49	TEK2K	I-2	165	146	15
21493784-1138285	LP758-43 (NLTT52182)	21 49 37.8	-11 38 29	TEK2K	A2-1	277	227	6

Coverage	ΔT	π_{rel}	μ_{rel}	P.A.	π_{abs}	V_{tan}	Pop. ^b	Notes ^c
(10)	(yr)	(mas)	(mas yr ⁻¹)	(deg)	(mas)	(km s ⁻¹)	(17)	(18)
1992.76-2002.62	9.86	6.26 ± 0.63	613.5 ± 0.2	180.8 ± 0.2	7.33 ± 0.63	397 ± 34	2	
2008.72-2017.00	8.28	1.22 ± 0.47	148.9 ± 0.1	108.5 ± 0.2	2.32 ± 0.48	304 ± 63	4	1
2003.72-2015.64	11.92	2.64 ± 0.34	230.3 ± 0.1	124.8 ± 0.2	3.84 ± 0.35	284 ± 26	2	
2010.75-2017.10	6.35	11.53 ± 0.56	765.7 ± 0.2	166.3 ± 0.2	12.77 ± 0.56	284 ± 12	2	2
2008.88-2017.10	8.22	5.95 ± 0.15	153.2 ± 0.1	205.1 ± 0.2	6.76 ± 0.16	107 ± 3	4	3
2008.29-2017.25	8.96	1.66 ± 0.26	237.7 ± 0.1	168.7 ± 0.2	2.47 ± 0.27	456 ± 50	4	
2012.94-2017.10	4.16	1.80 ± 0.59	66.5 ± 0.3	123.9 ± 0.3	2.86 ± 0.59	110 ± 23	1	
2004.05-2010.30	6.25	5.76 ± 0.45	62.6 ± 0.2	299.6 ± 0.3	6.70 ± 0.46	44 ± 3	1	
2008.29-2015.31	7.02	1.00 ± 0.39	120.1 ± 0.1	205.7 ± 0.2	1.66 ± 0.39	343 ± 81	2	
2003.18-2017.31	14.13	0.83 ± 0.30	87.7 ± 0.1	203.2 ± 0.2	1.77 ± 0.31	243 ± 45	2	1
2003.27-2016.45	13.18	1.29 ± 0.26	46.3 ± 0.1	240.0 ± 0.2	2.27 ± 0.27	100 ± 13	1	
2008.34-2017.49	9.15	3.34 ± 0.46	224.3 ± 0.1	267.2 ± 0.2	4.51 ± 0.47	236 ± 25	2	
2012.46-2017.49	5.03	6.76 ± 0.47	360.9 ± 0.2	259.9 ± 0.2	7.65 ± 0.47	224 ± 14	2	4
2003.19-2017.46	14.27	2.51 ± 0.32	41.1 ± 0.1	308.9 ± 0.2	3.53 ± 0.32	97 ± 5	1	
2008.25-2015.56	7.31	2.78 ± 0.39	141.7 ± 0.1	291.4 ± 0.2	3.98 ± 0.40	169 ± 17	3	
1992.20-2003.35	11.15	3.45 ± 0.41	281.1 ± 0.1	227.6 ± 0.2	4.70 ± 0.43	284 ± 26	2	
2003.48-2017.57	14.09	7.50 ± 0.20	187.4 ± 0.1	325.8 ± 0.2	8.99 ± 0.24	101 ± 5	4	3
2008.29-2015.54	7.25	1.57 ± 0.43	186.1 ± 0.1	308.7 ± 0.2	2.51 ± 0.43	583 ± 60	2	
2003.50-2010.72	7.22	9.09 ± 0.27	560.4 ± 0.1	150.7 ± 0.2	9.81 ± 0.27	271 ± 7	2	
2003.56-2017.97	14.41	6.18 ± 0.32	252.2 ± 0.1	89.8 ± 0.2	7.20 ± 0.33	166 ± 8	3	3

NOTE—Table 1 is published in machine-readable format.

^a Coordinates are from the 2MASS catalog.

^b Estimated Galactic population membership (see Section 3): (1) disk, (2) halo, (3) intermediate, (4) contradictory.

^c Notes on individual objects. (1) Hints of a possible very low amplitude perturbation not confirmed. (2) No evidence seen corresponding to the 245 day radial velocity period reported by Dearborn et al. (1986). (3) Tabulated astrometry after removal of the perturbation discussed in Section 2.4 below. (4) This is the common proper motion companion to 2MASS J14572616+2341227 (LSPM J1457+2341S) for which $\pi_{\text{abs}} = 5.77 \pm 1.48$ mas was reported in Dahn et al. (2017). These additional observations further support the physical nature of the pair. The weighted mean astrometric results for the pair are reported above. Kirkpatrick et al. (2016) reported evidence for a third component based on the ALLWISE motion survey.

Table 2. Photometric Results

2MASS J	<i>B</i>	<i>V</i>	<i>I</i>	Notes ^a	<i>J</i>	<i>H</i>	<i>K_S</i>
(1)	(2)	(3)	(4)	(5)	(6)	(7)	(8)
00260048–1918519	16.76 ± 0.05	15.07 ± 0.03	13.46 ± 0.03	1	12.540 ± 0.024	11.918 ± 0.026	11.587 ± 0.027
01202853–0836307	19.62 ± 0.05	17.72 ± 0.03	15.82 ± 0.03	1	14.990 ± 0.043	14.224 ± 0.048	13.665 ± 0.047
01215031+0113024	19.65 ± 0.05	17.76 ± 0.03	16.08 ± 0.03	1	15.107 ± 0.049	14.251 ± 0.045	13.805 ± 0.045
03323808+0157599	15.64 ± 0.01	13.89 ± 0.01	12.33 ± 0.01	2	11.470 ± 0.022	10.844 ± 0.024	10.480 ± 0.021
07425720+4659186	18.75 ± 0.05	16.65 ± 0.03	14.89 ± 0.03	1	13.520 ± 0.025	12.681 ± 0.026	12.182 ± 0.026
08180742+2234290	17.90 ± 0.15	16.24 ± 0.10	14.60 ± 0.10	3	13.744 ± 0.026	12.990 ± 0.026	12.634 ± 0.025
08345114+0740088	19.40 ± 0.15	17.28 ± 0.10	15.48 ± 0.10	3	14.416 ± 0.034	13.744 ± 0.040	13.426 ± 0.029
09332463–0031445	16.12 ± 0.05	14.64 ± 0.03	13.14 ± 0.03	1	12.190 ± 0.023	11.546 ± 0.024	11.335 ± 0.023
10542941+3402259	19.26 ± 0.15	17.79 ± 0.10	16.30 ± 0.10	3	15.501 ± 0.051	15.018 ± 0.065	14.655 ± 0.082
11203487+5559373	18.20 ± 0.05	16.66 ± 0.03	15.25 ± 0.03	1	14.408 ± 0.031	13.771 ± 0.043	13.633 ± 0.043
13533300–0040395	... ± ...	17.29 ± 0.03	15.60 ± 0.03	1	14.609 ± 0.036	13.798 ± 0.036	13.609 ± 0.051
14531880+6004209	19.95 ± 0.15	18.29 ± 0.10	16.49 ± 0.10	3	15.609 ± 0.054	15.053 ± 0.071	14.764 ± 0.092
14572597+2341257	19.37 ± 0.05	17.52 ± 0.03	15.63 ± 0.03	1	14.479 ± 0.040	13.745 ± 0.047	13.320 ± 0.039
15270276+4345172	... ± ...	16.89 ± 0.03	15.08 ± 0.03	1	14.002 ± 0.026	13.310 ± 0.026	13.021 ± 0.028
15480927+3227247	18.81 ± 0.15	17.19 ± 0.10	15.50 ± 0.10	3	14.495 ± 0.026	13.752 ± 0.032	13.464 ± 0.032
15523734+2927591	17.97 ± 0.05	16.30 ± 0.03	14.73 ± 0.03	1	13.797 ± 0.029	13.201 ± 0.035	12.881 ± 0.033
16223288+4237538	17.68 ± 0.05	16.24 ± 0.03	14.46 ± 0.03	1	13.288 ± 0.021	12.498 ± 0.021	11.899 ± 0.016
16313278+3553285	19.89 ± 0.15	18.13 ± 0.10	16.38 ± 0.10	3	15.466 ± 0.050	14.846 ± 0.060	14.326 ± 0.062
21051653+2514486	19.05 ± 0.05	17.42 ± 0.03	15.63 ± 0.03	1	14.481 ± 0.033	13.768 ± 0.030	13.191 ± 0.036
21493784–1138285	17.66 ± 0.05	15.83 ± 0.03	14.04 ± 0.03	1	13.002 ± 0.023	12.262 ± 0.023	11.898 ± 0.026

NOTE—Table 2 is published in machine-readable format.

^a Source of *BVI* photometry. (1) *BVI* from CCD measures on the NOFS 1.0 m telescope with estimated errors inflated to allow for significant differences between the spectral energy distributions of dwarf carbon stars and the photometric standard stars employed. (2) *BVI* from 17 independent measures on the NOFS 1.55 m telescope employing a single channel photoelectric photometer with instrumental response bandpasses well matched to the standard system. (3) *BVI* from SDSS *gri* data transformed to the Johnson-Cousins system via the relations presented by Ivezić et al. (2007, Table 7) and estimated errors inflated to allow for significant instrument bandpass differences.

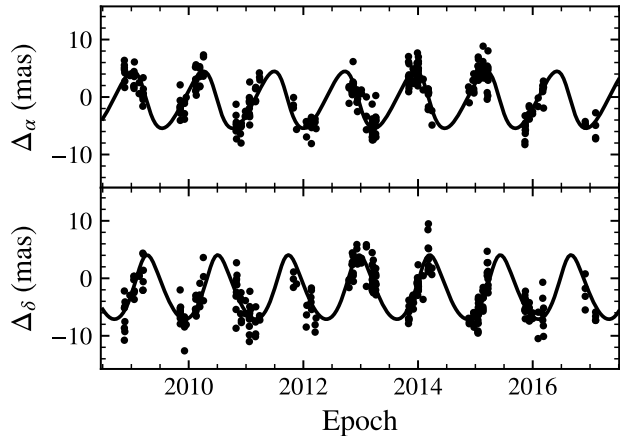


Figure 1. Positions in right ascension and declination for LSPM J0742+4659 after removing the parallactic and proper motions. The curves show the orbital-motion fit to these residuals as represented by the orbital elements given in Table 3.

out. The results for the parallax and proper motion are given in Table 1, and for the orbital motion are given in Table 3 and plotted in Figures 1 through 3. The eccentricity for all three orbits is quite small and, within the observational errors, is consistent with zero. A fourth target G77-61 has been found to be a spectroscopic binary (Dearborn et al. 1986), but we have not yet detected any significant signature of the orbit in the astrometric data. Another example of a dC spectroscopic binary was found among the SDSS carbon stars (Margon et al. 2018). It is notable for its short orbital period of 2.9 d, much shorter than that of G77-61 and the three new systems reported here. This short period implies a different orbital evolution during the mass-transfer process. Other spectroscopic binaries are being found in a new survey of dC stars (Whitehouse et al. in preparation).

3. DISCUSSION

Studies by McClure and others (McClure & Woodsworth 1990; McClure 1997) have shown that the subgiant CH, giant CH, and giant Ba stars are all binaries, most with periods 400 – 4000 days and with eccentricities smaller than

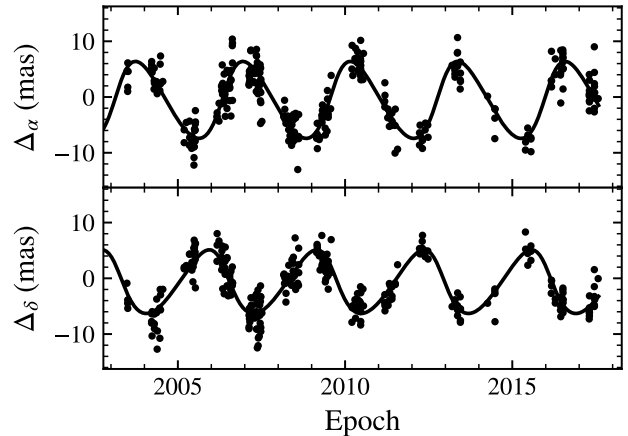


Figure 2. Same as Figure 1, for LP225-12.

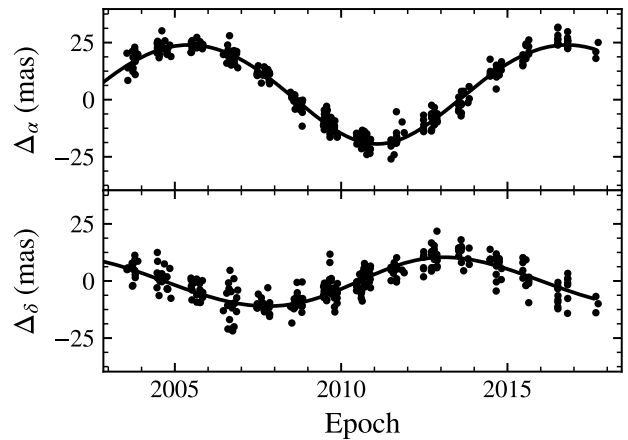


Figure 3. Same as Figure 1, for LP758-43.

for normal binaries. These facts indicate a previous phase of orbital dissipation during mass transfer from an AGB companion, likely during wind accretion from the companion.

The orbits of the three dC binaries in this paper are consistent with this picture. The three binaries have periods 450–4100 days, and their eccentricities are small. Using the parallaxes in Table 1, the amplitudes of the photocenter orbits in Table 3 are 0.9, 1.6, and 3.1 AU. The true orbits will be larger if the secondary star is contributing significant light to the photocenter. Because the data are taken with a red filter (the wide-R A2-1 filter for LP758-43, and I-2 for the other two binaries), and the companions

Table 3. Orbits of New Astrometric dC Binaries

Parameter	LSPM J0742+4659	LP225-12	LP758-43
Period (yr)	1.23 ± 0.01	3.21 ± 0.01	11.35 ± 0.15
α^a (mas)	5.83 ± 0.54	14.21 ± 0.41	22.09 ± 0.14
i (deg)	150 ± 4	72 ± 2	63.3 ± 1.0
e	0.3 ± 0.2	0.3 ± 0.2	0.1 ± 0.1
ω (deg)	132 ± 20	270 ± 15	350 ± 20
Ω (deg)	154 ± 5	128.5 ± 0.5	282 ± 3
T_0	2014.1 ± 0.1	2006.5 ± 0.5	2011.0 ± 0.5

^aSemimajor axis of the photocentric orbit.

are likely to be white dwarfs, we expect that not much light is contributed by the companions. These amplitudes are comparable to those for the CH and Ba stars studied by McClure, and similar to the maximum size of the AGB star thought to be the source of the carbon-rich material transferred to the dC star we see now.

The binaries found in this paper are expected to be those with long periods among nearby targets, because they will have the largest apparent (angular) orbits that are easiest to detect astrometrically. It is likely that more binaries with smaller astrometric amplitudes are undetected in our sample. Indeed, the high frequency of binaries being found using radial velocities (Whitehouse et al. in preparation) indicates that most or all dC stars are now in binaries with white dwarf companions. Further study, and the determination of their orbits, can confirm this expectation.

Figure 4 shows that the stars in this sample have $J - K_S$ colors redder than oxygen-rich dwarfs and subdwarfs. Presumably, their J -band flux is suppressed by CN absorption, although some contribution from K_S -band brightening from dust emission in a few stars is possible. The subdwarf LHS466, taken from Dahn et al. (2017), has $J - K_S = 0.88$ measured by 2MASS, suggesting it might be the brightest known dC star. However, its UKIDSS $J - K_S =$

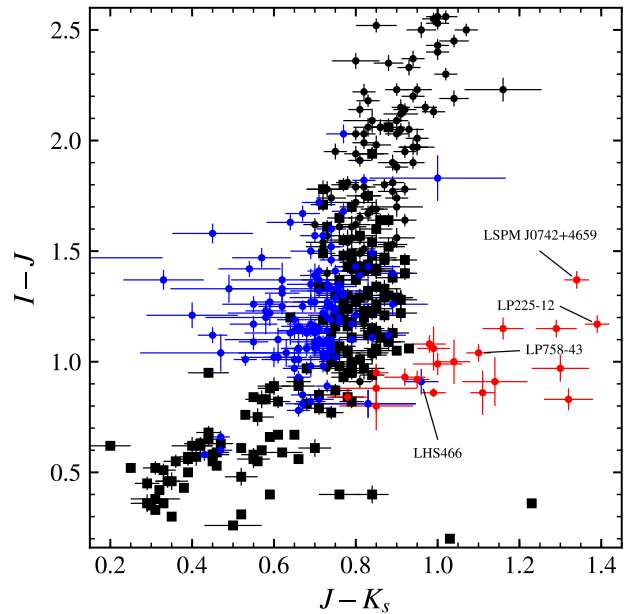


Figure 4. $I - J$ versus $J - K_S$ for the dwarf carbon stars in this paper (red circles), along with late K and M dwarf (black circles) and subdwarf stars (blue circles) from Dahn et al. (2017), as well as selected late dwarf stars with parallaxes from *Hipparcos* and good *VI* and 2MASS photometry (black squares).

0.64, corresponding to 0.66 on the 2MASS system, indicates the 2MASS value is spurious or contaminated. Therefore, Figure 4 appears to provide a nearly clean separation of our dC stars.

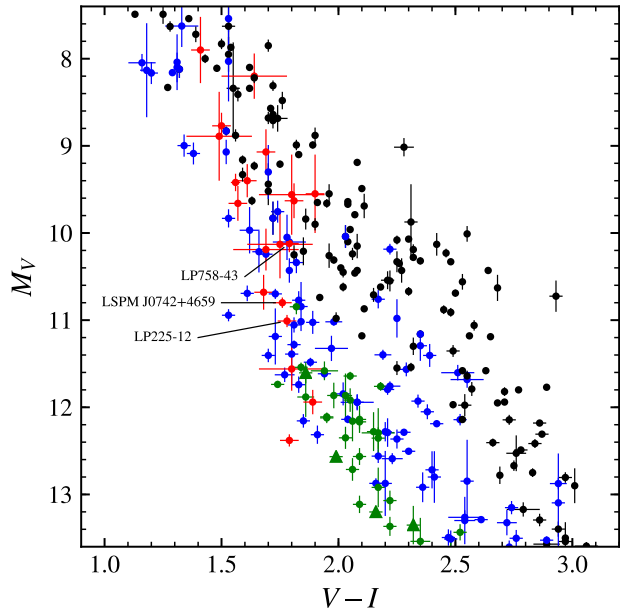


Figure 5. M_V versus $V - I$ for the dwarf carbon stars in this paper (red circles). The three new astrometric dC binaries are noted. Additional data points include late K and M dwarf (black circles) and subdwarf stars (blue circles) from Dahn et al. (2017) and *Hipparcos*. Also plotted are extreme subdwarf (green circles) and ultra subdwarf (green triangle) M stars from Dahn et al. (2017).

Using $J - K_S$ colors to separate dC stars from the far more common oxygen-rich dwarfs may provide an important means of identifying a complete sample of dC stars in the solar neighborhood. This step will be necessary to avoid the selection effects in the present discovery of dC stars from SDSS, and thus in the sample in this paper. Therefore, Figure 4 may provide a procedure to utilize Gaia data for an expanded sample to facilitate understanding the true range of properties of these stars.

Figure 5 shows a color-absolute magnitude diagram of the stars in this paper. They cover a range of M_V of 7.9–12.4, and are subluminescent by up to 3 mag in M_V . We see that the close agreement of M_V for the first 3 dCs with parallaxes (Harris et al. 1998) was apparently fortuitous. Using the degree of subluminescence in Figure 5, together with their tangential veloci-

ties from Table 1, we can classify each star as probable disk or halo (Column 17 in Table 1).¹ We find four stars are probable disk, 10 stars are probable halo, two stars have intermediate values of subluminescence and velocity, and four stars have contradictory values. This result confirms that the dC stars do have a wide range of properties, with origins in the disk as well as the halo (Farihi et al. 2018).

The first dwarf carbon star (G77-61) was identified as a dwarf from its parallax as measured by the USNO plate parallax program (Dahn et al. 1977). 40 years later, parallaxes have been measured for only 20 additional dwarf carbon stars, all by the USNO CCD parallax program, including the 20 presented in this paper. Gaia DR2 will probably have parallax data for most of the stars in this paper (Katz & Brown 2017). The faintest stars may have $G > 20$, fainter than the limit for DR2, and a few are likely to have a binary perturbation detected by Gaia, and will be omitted from DR2 until a later data release. For the stars that are in DR2, the formal error of the DR2 parallaxes is estimated to be 0.1 – 0.7 mas for the magnitude range of our dC sample. Therefore, DR2 data probably will improve on the conclusions of this paper, other than the topic of binary perturbations that DR2 will not address. Later data releases from Gaia will certainly improve on the distances, the bi-

¹ Neither the tangential velocity nor the “subluminescence” in Figure 5 are necessarily reliable indicators of the population of a star. Halo stars can by chance have a small tangential velocity, and disk stars can acquire high velocities through dynamical interactions. The high-velocity dC star found by Plant et al. (2016) is discussed as possibly having acquired its high velocity by ejection from a binary. Stars positions in Figure 5 are affected by the distorted spectral energy distribution of dC stars, most importantly by absorption in V by the C_2 Swan bands that shift $V - I$ toward a redder color for stars with strong bands. A diagram plotting luminosity versus temperature would be preferable.

nary characteristics, and the sample size available to understand dC stars.

This publication makes use of data products from the Two Micron All Sky Survey, which is a

joint project of the University of Massachusetts and the Infrared Processing and Analysis Center/California Institute of Technology, funded by the National Aeronautics and Space Administration and the National Science Foundation.

REFERENCES

- Dahn, C. C., Liebert, J., Kron, R. G., Spinrad, H., & Hintzen, P. M. 1977, *ApJ*, 216, 757
- Dahn, C. C., Harris, H. C., Subasavage, J. P., et al. 2017, *AJ*, 154, 147
- Dearborn, D. S. P., Liebert, J., Aaronson, M., et al. 1986, *ApJ*, 300, 314
- Downes, R. A., Margon, B., Anderson, S. F., et al. 2004, *AJ*, 127, 2838
- Farihi, J., Arendt, A. R., Machado, H. S., & Whitehouse, L. J. 2018, *MNRAS*, arXiv:1804.01989
- Fukugita, M., Ichikawa, T., Gunn, J. E., et al. 1996, *AJ*, 111, 1748
- Green, P. 2013, *ApJ*, 765, 12
- Green, P. J., & Margon, B. 1994, *ApJ*, 423, 723
- Gunn, J. E., Carr, M., Rockosi, C., et al. 1998, *AJ*, 116, 3040
- Gunn, J. E., Siegmund, W. A., Mannery, E. J., et al. 2006, *AJ*, 131, 2332
- Harris, H. C., Dahn, C. C., Walker, R. L., et al. 1998, *ApJ*, 502, 437
- Ivezić, Ž., Smith, J. A., Miknaitis, G., et al. 2007, *AJ*, 134, 973
- Katz, D., & Brown, A. G. A. 2017, in *SF2A-2017: Proceedings of the Annual meeting of the French Society of Astronomy and Astrophysics*, ed. C. Reylé, P. Di Matteo, F. Herpin, E. Lagadec, A. Lançon, Z. Meliani, & F. Royer, 259–263
- Kirkpatrick, J. D., Kellogg, K., Schneider, A. C., et al. 2016, *ApJS*, 224, 36
- Margon, B., Kupfer, T., Burdge, K., et al. 2018, *ApJL*, 856, L2
- Margon, B., Anderson, S. F., Harris, H. C., et al. 2002, *AJ*, 124, 1651
- McClure, R. D. 1997, *PASP*, 109, 536
- McClure, R. D., & Woodsworth, A. W. 1990, *ApJ*, 352, 709
- Monet, D. G., Dahn, C. C., Vrba, F. J., et al. 1992, *AJ*, 103, 638
- Plant, K. A., Margon, B., Guhathakurta, P., et al. 2016, *ApJ*, 833, 232
- Skrutskie, M. F., Cutri, R. M., Stiening, R., et al. 2006, *AJ*, 131, 1163
- Whitehouse, L. J., Farihi, J., Subasavage, J. P., et al. in preparation, ,
- York, D. G., Adelman, J., Anderson, Jr., J. E., et al. 2000, *AJ*, 120, 1579

Facility: USNO:61in (TEK2K, EEV24), USNO:40in, Sloan